# A Description of the Geological Context, Discrete Traits, and Linear Morphometrics of the Middle Pleistocene Hominin from Dali, Shaanxi Province, China

Xinzhi Wu[1] and Sheela Athreya[2]*

[1]*Laboratory for Human Evolution, Institute of Vertebrate Paleontology and Paleoanthropology, Chinese Academy of Sciences, Beijing 100044, China*
[2]*Department of Anthropology, Texas A&M University, College Station, TX 77843*

ABSTRACT    In 1978, a nearly complete hominin fossil cranium was recovered from loess deposits at the site of Dali in Shaanxi Province, northwestern China. It was subsequently briefly described in both English and Chinese publications. Here we present a comprehensive univariate and nonmetric description of the specimen and provide comparisons with key Middle Pleistocene *Homo erectus* and non-*erectus* hominins from Eurasia and Africa. In both respects we find affinities with Chinese *H. erectus* as well as African and European Middle Pleistocene hominins typically referred to as *Homo heidelbergensis*. Specifically, the Dali specimen possesses a low cranial height, relatively short and arched parietal bones, an angled occipital bone, and a nonprominent articular tubercle relative to the preglenoid surface all of which distinguish it from Afro/European Middle Pleistocene *Homo* and align it with Asian *H. erectus*. At the same time, it displays a more derived morphology of the supraorbital torus and supratoral sulcus and a thinner tympanic plate than *H. erectus*, a relatively long upper (lambda-inion) occipital plane with a clear separation of inion and opisthocranion, and an absolute and relative increase in brain size, all of which align it with African and European Middle Pleistocene *Homo*. Finally, traits such as the form of the frontal keel and the relatively short, broad midface align Dali specifically with other Chinese specimens from the Middle Pleistocene and Late Pleistocene, including *H. erectus*, and differentiate these from the Afro/European specimens of this time period. Am J Phys Anthropol 150:141–157, 2013.    © 2012 Wiley Periodicals, Inc.

Middle Pleistocene hominin evolution in Eurasia and Africa is characterized in part by the appearance of so-called "transitional" fossils that exhibit a combination of archaic (in particular *Homo erectus*) and derived traits. The taxon *Homo heidelbergensis* is generally accepted as being applicable to some of these specimens (Mounier, 2009; Stringer, 2012), but the issue of interregional variation makes it difficult to determine exactly to which groups this term should apply. In particular, researchers are unclear on the position of the non-*erectus* Middle Pleistocene fossils from Asia—namely the Narmada fossil from India and the Dali, Jinniushan, and Maba specimens from China—and agree that further analysis is needed, particularly of the Chinese specimens (Athreya, 2007; Rightmire, 2007, 2008; Hublin, in press).

Of the above named fossils, the most complete and therefore arguably the most important in elucidating the systematic position of East Asian Middle Pleistocene *Homo* is the Dali hominin from China (Figs. 1–6). It was found in 1978 in a gravel layer of loess deposits along the Luo He (or Luo River) near Jiefang Village in Dali County, Shaanxi Province, northwestern China (34° 52′ N, 109° 40′ E) (Fig. 7). The original report of the discovery was published by Wang et al. (1979) in Chinese. Subsequent detailed assessments were provided in English by Wu (1981, 2009) and Wu and Poirier (1995).

Here we report a compilation of these data, and include additional metric and nonmetric assessments of the specimen. Using linear craniometrics and a visual assessment of certain nonmetric traits, we describe the morphology of Dali in a comparative context. A more detailed multivariate morphometric analysis of Dali relative to a larger comparative sample, using primary data, is forthcoming (Athreya and Wu, in preparation). Therefore, the main intent of this report is to provide a detailed overall description of Dali, and to contextualize the morphology of this key specimen relative to a handful of relatively complete penecontemporaneous fossils from Europe, Asia, and Africa. In particular, we are interested in presenting the morphology of Dali in the context of other Middle Pleistocene groups—namely Asian *H. erectus*, *H. heidelbergensis* as defined by Rightmire (2004, 2007, 2008), and other Middle and Late

**Fig. 1.** Frontal views of the Dali specimen [Color figure can be viewed in the online issue, which is available at wileyonlinelibrary. com.].
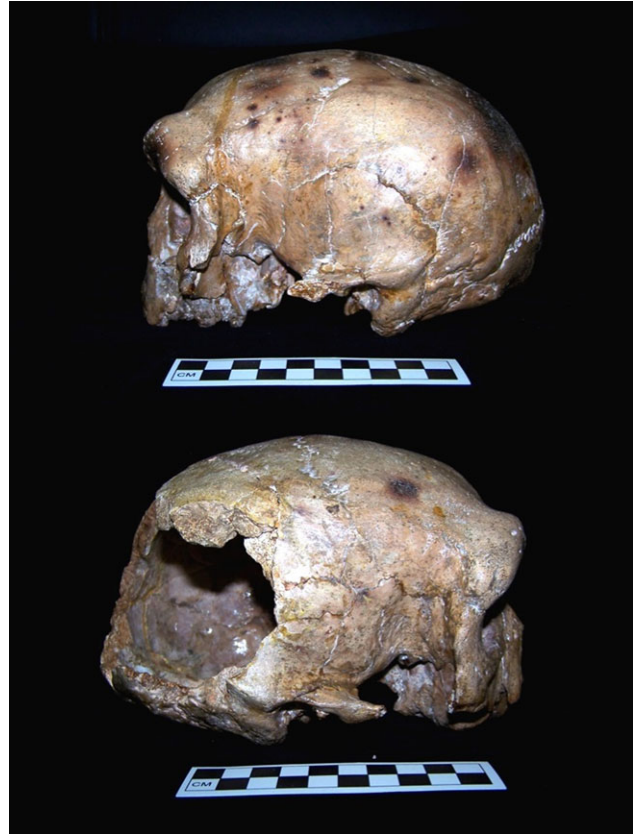


**Fig. 2.** Lateral views of the Dali specimen. [Color figure can be viewed in the online issue, which is available at wileyonlinelibrary. com.]

Pleistocene specimens from China such as Maba, Jinniushan, and the Zhoukoudian Upper Cave fossils.

## SETTING AND GEOLOGICAL CONTEXT OF THE DALI DISCOVERY

The Dali cranium was discovered in 1978 by Chinese geologist Liu Shuntang working in the western part of Dali County in the Shaanxi Province of northwestern China. The site is located near the southern edge of the Chinese Loess Plateau, situated near the Luo He (Luo River) which is a tributary of the Wei He (Wei River) and secondary tributary of the Huang He (Yellow River) (Fig. 7). The sedimentary sequence of the site consists of thirteen layers, with the Dali specimen found in Layer 3, which is the third of three alluvial terraces that have formed along the Luo River (Fig. 8). The specimen was situated on top of a gravel unit made up of fluvial sediments overlain by sandy and silty sediments, and it was recovered about 33 m below the top surface of the terrace and 45 to 50 m above the present-day river (Xiao et al., 2002). The lower portion of the profile consisting of Layers 1 to 9 is fluviatile in origin, and Layers 10 to 13 are loess deposits. Subsequent excavations yielded stone artifacts and both vertebrate and invertebrate fauna from the same gravel bed (Wu and You, 1979).

The age of Dali has been inferred based on the direct dating of associated material by several different methods, all providing relatively consistent results (Supporting Information/SI Table 1). The preponderance of



**Fig. 3.** Close up of pathological lesion on left parietal. [Color figure can be viewed in the online issue, which is available at wileyonlinelibrary.com.]

faunal data indicates that the level from which the Dali specimen derives dates to the late-Middle Pleistocene and is likely between 200 and 250 ka. However, there is some debate over the extent to which the specimen was in a primary vs. secondary depositional context. Pope (1992) provided a detailed review of these data. He noted that the abraded condition of some of the artifacts and faunal remains, as well as the presence of fish fossils

**Fig. 4.** Occipital view of the Dali specimen. [Color figure can be viewed in the online issue, which is available at wileyonlinelibrary. com.]

and river gravels, strongly indicated a certain amount of fluvial transport. However, the condition and preservation of the cranium suggest that it was minimally transported. Nonetheless, the gravel matrix in which the fossil was found raises questions as to the contemporaneity of the faunal remains with the hominin fossil. Thus, despite the repeatability of the ages of the associated faunal remains, their relationship to the age of the Dali specimen remains unclear.

The geological data appear to be more secure, with initial TL dates on paleosols above the specimen providing a minimum age of 41 to 71 ka (Wang et al., 1979). Subsequent analyses correlated the loess deposits of the Dali site (Layers 10–13) to L1 and L2 of the Chinese loess sequence and the two paleosols to S1 and S2. Specifically, the fossil-bearing unit (Layer 3) is 13 meters below the level of a paleosol that corresponds with the S2 unit of the Chinese loess sequence, placing the minimum age of the fossil at MIS 7 or ca. 247 ka (Kukla, 1987; Qi, 1989; Heslop et al., 2000; Yin et al., 2002). Chronostratigraphic dating of the loess-paleosol sequence at the Dali site confirmed a slightly older age, placing it at 270 ka (Xiao et al., 2002). We thus concur with Pope (1992) that it is reasonable to accept a minimum age of ca. 250 ka for the specimen.

Over 15 species of fauna were recovered from the site including several that indicate a terminal Middle Pleistocene biostratigraphic age based on correlations with other localities (Wang et al., 1979; Wu, 1981; Zhang and Zhou, 1984). Keates (2003) noted that the species identification of many of these is uncertain, but the assemblage includes *Palaeoxodon* sp., *Equus* sp., *Rhinoceros* sp., *Megaloceros pachyosteus*, *Pseudaxis* cf. *grayi*, and *Bubalus* sp. The fauna indicate a mix of warmer and cooler adapted species. Namely, the presence of *Palaeoloxodon* suggests a subarctic climate while the *Megaloceros pachyosteus* and *Pseudaxis grayi*, among others, indicate temperate open woodland. Given the site's locality at the boundary between the so-called Palearctic



**Fig. 5.** Superior view of the Dali specimen. [Color figure can be viewed in the online issue, which is available at wileyonlinelibrary. com.]

(Northeast Asian) and Oriental (Southeast Asian) biogeographic zones (but see Norton et al., 2010), this mix of fauna is not surprising and suggests that the region experienced variable warmer and cooler periods during the Middle and Late Pleistocene. This is supported by several faunal assemblages in the region such as at Lantian, which show that the grassland forms typical of the Early Pleistocene were enhanced by the appearance of woodland forms migrating from South China during the Middle Pleistocene (Jin et al., 1999). The presence of *Palaeoloxodon*, *Equus*, *Rhinoceros*, *Megaloceros pachyosteus*, and *Pseudaxis* cf. *grayi* support this inference, all of which are found in both northeastern and southeastern Chinese sites during the Middle Pleistocene.

The archaeological remains associated with the fossil consist of over 180 small stone artifacts (Wu and Poirier, 1995). Typologically, the assemblage is comprised mainly of scrapers, points and burins. These would correspond primarily with Mode 1 tools defined elsewhere in the Old World, although as has been pointed out by several scholars (Schick and Zhuan, 1993; Gao, 1999; Gao and Norton, 2002; Wu, 2004), the Paleolithic sequence in China does not correspond with that of regions to the west, where a succession from Mode 1 to Mode 5 occurred throughout the Pleistocene.

## PRESERVATION AND ONTOGENETIC AGE

The Dali cranium is fairly well-preserved although no upper dentition, mandibular, or postcranial remains are

preserved (Figs. 1–6). The right part of the posterior vault is lost, affecting portions of the parietal, temporal, and occipital bones. The posterior and inferior parts of the left zygomatic, the lower part of nasal bones, and part of both orbital roofs are also missing. A certain amount of postdepositional distortion is present. Namely, the lower portion of both maxillary bones and the hard palate are slightly displaced superiorly affecting measurements that include the palate such as upper facial height. The frontal processes of the maxilla are bilaterally intact and the neurocranium is undistorted.

Past studies (Wu, 1981; Pope, 1992) have cited the thicknesses of the brow ridge and cranial wall, the robustness of the temporal lines, muscular markings on the nuchal plane of the occipital, and the robustness of the supramastoid ridge to suggest the sex of the Dali individual to be male. In addition, the roughly contemporaneous Jinniushan fossil is more gracile and, based on pelvic morphology, is female (Rosenberg et al., 2006). The differences in robusticity between the two specimens further support a male attribution for Dali. However, given the near impossibility of sexing fossil crania, the sex of the Dali individual cannot be unequivocally assessed without a more complete contemporaneous comparative sample.

Dali's pattern and degree of suture closure on the outer surface of the cranial vault indicate an adult age for the specimen. All of the ectocranial sutures are visible except the sphenofrontal suture on the left side. The spheno-occipital synchondrosis is fused but visible. Endocranially, there is no suture obliteration. Based on these indicators, the specimen falls in the young adult category (25–49 years of age) following Steele and Bramblett (1988). It should be noted that there are considerable problems using suture closure to estimate age for fossils such as this, since the reference samples are both modern and of non-Asian ancestry and no other indicators such as dentition or postcrania are available (McKern and Stewart, 1957; Meindl and Lovejoy, 1985; Key et al., 1994). Therefore, this estimation cannot be narrowed further, although given the absence of suture obliteration, particularly the basilar suture, it is reasonable to expect the age at death for the Dali individual to fall at the lower end of the 25 to 49 years range.
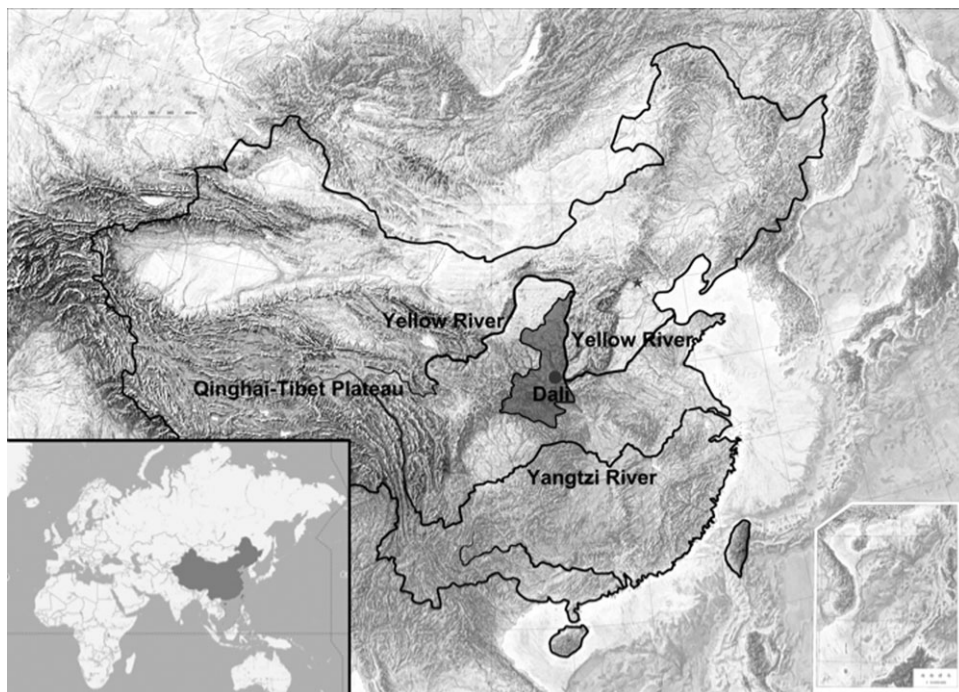


**Fig. 6.** Basal view of the Dali specimen. [Color figure can be viewed in the online issue, which is available at wileyonlinelibrary.com.]
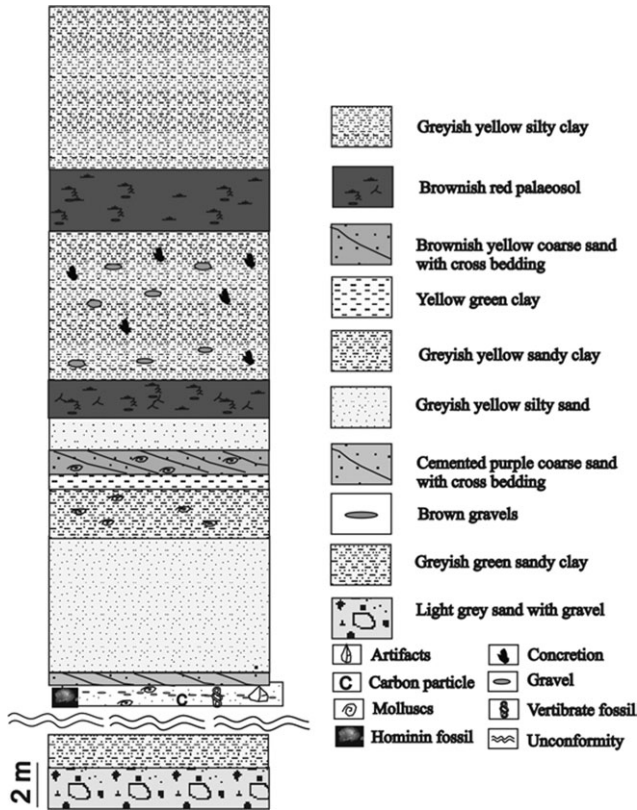


**Fig. 7.** Map of Dali locality.

**Fig. 8.** Geological profile of Dali locality.

## Paleopathology

The Dali specimen possesses a small lesion on the posterior portion of the left parietal bone near the lambdoid suture (Fig. 3). The lesion is a roughly rhomboid-shaped, shallow depression partly surrounded by a slight proliferation of bone. The long axis of the depression extends superolaterally to infero-medially. The length and breadth are approximately 18 mm and 14 mm, respectively. The position of the lesion indicates that it is subcutaneous. It is not located in the area that would have been covered by masticatory or nuchal musculatures and there is no evidence of endocranial change in the vicinity of the lesion. Remodeling is present, indicating that it occurred antemortem. Similar lesions have been reported from Atapuerca's Sima de los Huesos (SH) site with high frequency (Pérez et al, 1997). In addition, specimens from several sites in Asia including Zhoukoudian, Maba, and three cranial fragments from Xujiayao exhibit antemortem cranial lesions, indicating that survival of cranial trauma was not uncommon among archaic hominins from this region (Wu et al, 2011; Wu and Trinkaus, in press).

## MATERIALS AND METHODS

The Dali specimen was compared to a sample of Middle and Late Pleistocene specimens which were chosen based on their completeness, ontogenetic age, and geological age. The main comparative samples are Chinese *H. erectus* and the non-*erectus* Middle Pleistocene sample. Since sufficient debate exists around the hypodigm of *H. heidelbergensis* (Tattersall and Schwartz, 2006;

Rightmire, 2008; Athreya, 2010; Hublin, in press) we refrain from using that term here, and refer to it as the Afro/European Middle Pleistocene (MP) group. We also include the Ngandong specimens since they have recently been redated and could be penecontemporaneous with the African and European MP samples, dating to some time within the last 500 ka (Indriati et al., 2011). Table 1 provides a complete list of measurements for Dali. Further details on the specific individuals included in the comparative sample, as well as the rationale for group configurations, can be found in the Supporting Information (SI Tables 2 and 3 ).

Linear measurements were collected on the original Dali specimen using conventional sliding, spreading, and coordinate calipers. Each measurement was taken at least three times over the course of several days by XW, and the average values were used here. Measurement protocols followed that of Martin and Saller (1957) as well as Howells (1973) as defined in his monograph. Bräuer (1988) was also used for measurement definitions, particularly when reconciling minor differences between the protocols of Martin and Saller versus Howells.

## MORPHOLOGICAL DESCRIPTION
### Frontoparietal region

The frontal bone of Dali is complete and undistorted (Fig. 1). The facial portion of the bone is characterized by a prominent and vertically thick supraorbital torus that is shaped by arches over each orbit separated at glabella. Each arch has a smoothly curved inferior border and a superior border that is arched and angular, particularly above the central portion of each orbit. The thickest segment above each orbit is in the central portion, which measures 22.0 mm and 20.0 mm thick on the left and right sides, respectively. The medial segment is 19.0 mm on both sides, and the lateral segment of the torus is 15.0 mm on the left and 14.0 mm on the right side. The frontal bone is quite prominent and swollen at glabella relative to both the naso-frontal suture inferiorly and the neurocranial vault superiorly. However, lateral to glabella the medial portion of each browridge is swollen such that glabella appears less prominent or to be in somewhat of a "depression" relative to the horizontal plane of the supraorbital torus. The supraorbital torus remains thick at the zygomatic process. A supraorbital trigone (sensu Cunningham, 1908) is present. The zygomatic process of the frontal is noticeably thicker than the frontal process of the zygomatic with which it articulates. The inferior margin of the torus is rounded versus sharp, the latter of which is typical of the Zhoukoudian (ZKD) *H. erectus* (Weidenreich, 1943). Unlike the Zhoukoudian specimens, no supraorbital notch or foramen is present on Dali.

The supraorbital torus is separated from the frontal squama by a weak sulcus. In the metopic region Dali possesses a fusiform, narrow-based keel that begins about 23 to 25 mm above glabella and extends about 50 mm, attenuating towards the posterior and anterior ends. This ridge is considered a metopic versus a sagittal keel because it is anteriorly positioned and does not continue or connect with the bregmatic eminence, the latter of which is very weak. The bregmatic eminence is rhomboidal in shape, about 50 to 60 mm long in the antero-posterior direction and extending approximately 24 mm behind the coronal suture. It is so faint that it can easily be neglected during casual observation. For example, it

*TABLE 1. Craniofacial measurements for Dali*

| Measurement (Howells abbreviation, Martin number, and definition, or citation) | Value for Dali (mm unless otherwise indicated) |
|---|---|
| **Whole cranial vault** | |
| Maximum cranial length (GOL/M1, g-op) | 206.5 |
| Nasio-occipital length (NOL/M1d/n-op) | 196.5 |
| Glabella-inion length (M2/g-i) | 190 |
| Basion-nasion length (BNL/M5, ba-n) | 105.5 |
| Nasion-opisthion length (M5(1)/n-o) | 143 |
| Maximum cranial breadth (XCB/M8, eu-eu) | 149.5 |
| Maximum cranial breadth at supramastoid crest | 150.5 |
| Biauricular breadth (AUB/M11, au-au) | 141 |
| Minimum cranial breadth (WCB/M14, it-it) | 79 |
| Basion-bregma height (BBH/M17, ba-b) | 118 |
| Auriculo-bregmatic height (M20/po-b) | 102.5 |
| Horizontal circumference (M23/g-op-g) | 580 |
| Transverse cranial arc (M24/po-b-po arc) | 299 |
| Total sagittal arc (M25/n-o arc) | 379 |
| Basion-prosthion length (BPL/M40, ba-pr) | (105) |
| Biporion breadth (po-po) | 133 |
| **Frontal bone** | |
| Least frontal breadth (WFB/M9, ft-ft) | 104 |
| Minimum frontal breadth at temporal lines | 104 |
| Maximum frontal breadth at temporal lines | 111 |
| Maximum frontal breadth (XFB/M10, co-co) | 119 |
| Frontal sagittal arc (M26/n-b arc) | 135 |
| Frontal sagittal chord (FRC/M29, n-b chord) | 114 |
| Nasion-subtense fraction (FRF/M29c) | 49 |
| Lower frontal inclination angle (m-g-i) | 72° |
| Frontal inclination angle (M32(1), b-n-i) | 54° |
| Bregma angle (M32(2), b-g-i) | 50° |
| Frontal angle (FRA/M32(5)) | 128° |
| Bi-frontomalare temporale breadth (FMT/M43, fmt-fmt) | 121 |
| Bifrontal breadth (FMB, M43a, fm:a-fm:a) | 114 |
| Supraorbital torus thickness (central) (SOT) (Rightmire et al., 2006) | 22(l)/20(r) |
| SOT (lateral) (Rightmire et al., 2006) | 15(l)/14(r) |
| SOT (medial) | 19(l)/19(r) |
| **Parietotemporal region** | |
| Total length of temporal (M4a) | 89 |
| Bistephanic breadth (STB/M10b, st-st) | 110 |
| Biasterion breadth (ASB/M12, ast-ast) | 115 |
| Mastoid height (MDH/M19a) | 26.5 |
| Mastoid breadth (MDB/M13a, ms-ms) | 13 |
| Parietal sagittal arc (M27, b-l arc) | 115[a] |
| Bregma-sphenion arc (M27(2), b-sphn arc) | 103.5 |
| Lambda-asterion arc (M27(3), l-ast arc) | 105[a] |
| Parietal sagittal chord (PAC/M30, b-l chord) | 107[a] |
| Bregma-sphenion chord (M30(2), b-sphn) | 91.2 (l)/88.6 (r) |
| Lambda-asterion chord (M30(3), l-ast) | 100/92[a] |
| Parietal angle (PAA/M33e) | 147° |
| Temporal squama height (Martínez and Arsuaga, 1997) | 46.5 |
| Temporal squama length (Martínez and Arsuaga, 1997) | 72 |
| Temporal squama angle (Martínez and Arsuaga, 1997) | 65° |
| Bregma-asterion chord (BAC/M30c, b-ast) | 131 |
| Maximum biparietal breadth (Rightmire et al., 2006) | 149.5 |
| **Occipital bone** | |
| Foramen magnum length (FOL/M7, ba-o) | 38 |
| Foramen magnum breadth (M16) | 28 |
| Occipital sagittal arc (M28, l-o arc) | 128[a] |
| Lambda-inion arc (M28(1), l-i arc) | 91[a] |
| Inion-opisthion arc (M28(2), i-o arc) | 40 |
| Occipital sagittal chord (OCC/M30, l-o) | 91[a] |
| Lambda-inion chord (LIC/M31(1), l-i) | 74[a] |

*TABLE 1. (Continued)*

| Measurement (Howells abbreviation, Martin number, and definition, or citation) | Value for Dali (mm unless otherwise indicated) |
|---|---|
| Inion-opisthion chord (IOC/M31(2), i-o) | 39 |
| Occipital angle (OCA/M33d) | 96° |
| Lambda-inion-opisthion angle (M33(4), l-i-o) | 105° |
| Occipital height (l-sphba) | 117 |
| Inion-endinion | 11 |
| **Facial skeleton** | |
| Nasio-frontal subtense (NAS/M43b) | 18.8 |
| Bijugal breadth (JUB/M45(1), ju-ju) | (128) |
| Nasion-prosthion height (NPH/M48, n-pr) | (75) |
| Biorbital breadth (EKB/M44, ek-ek) | 110 |
| Bizygomatic breadth (ZYB/M45, zy-zy) | (141) |
| Cheek height (WMH/M48d) | 23 |
| Interorbital breadth (DKB/M49a, d-d) | 26 |
| Anterior interorbital breadth (IOW/M50, mf-mf) | 21 |
| Orbital breadth (M51, mf-ek) | 45 (r) |
| Orbital height (OBH/M52) | 34 (r) |
| Nasal breadth (NLB/M54) | 33 |
| Nasal height (NLH/M55, n-ns) | (53) |
| Nasio-frontal angle (NFA/M77a, fm:a-n-fm:a) | 143° |
| Maximum malar height (Rightmire et al., 2006) | 53 |

Values in parentheses are estimates.
[a] Represents the measurement taken by extending the trend of the preserved portion of the left lambdoidal suture to locate lambda.

was not noted in the description of the Dali specimen by Schwartz and Tattersall (2003).

Dali has a relatively low frontal index of 84.4 (nasion-bregma chord/arc × 100) (Bräuer, 1988) indicating that it has a relatively short and arched frontal. The frontal squama rises above and slopes backwards behind the supraorbital torus from a relatively shallow supratoral sulcus. The nasion-subtense fraction: nasion-bregma chord index (M29c/M29 × 100) (Martin and Saller, 1957) provides an indication of the position of the most prominent aspect of the midsagittal profile (Supporting Information SI Table 4 ). All values below 50 including Dali's value of 42.9 indicate that the most prominent aspect is located on the lower half of the frontal squama. Notably, all Chinese specimens have a value below 50. The minimum frontal breadth (ft-ft) is 104.0 mm, and the postorbital constriction index using the definition of Kimbel et al. (1984) of minimum frontal breadth/bifrontomalare temporale × 100 yields a value of 85.9. Following Rightmire's (1990) definition of the postorbital constriction index (minimum frontal breadth/biorbital chord or FMB), Dali's value is 91.2. From the postorbital region, the frontal bone expands continuously but modestly to the coronal suture. The minimum and maximum frontal breadths at the temporal lines are 104.0 mm and 111.0 mm, respectively, although at its broadest the maximum frontal breadth is 119.0 mm.

A significant portion of the right parietal bone is missing on Dali, and the left is slightly damaged in the posterior-medial section (Fig. 2). But because of the near completeness of the left, it is possible to reconstruct most of the right through mirror imaging and assessing the fit of the adjacent bones. While this is an imperfect approach given that it assumes perfect bilateral symmetry—which is often not the case—we employ it for the purposes of obtaining reasonable estimates of biparietal measurements. The parietal is relatively short and arched, more

*TABLE 2. Comparison of nonmetric traits between Dali, Afro/European Middle Pleistocene Homo and Asian H. erectus*

| Character | Dali | Afro/European MP *Homo* | Chinese *H. erectus* | Ngandong *H. erectus* | Additional references |
|---|---|---|---|---|---|
| SO torus configuration | Arched over each orbit | Arched over each orbit | Arched over each orbit | Straight bar of bone | Rightmire, 1998; Antón, 2003 |
| Supraorbital torus divided into distinct medial and lateral portions | Yes | Yes | No | No | |
| SO torus pneumatization | Not heavily pneumatized | Heavily pneumatized | Not heavily pneumatized | Not heavily pneumatized | Weidenreich, 1943, 1951; Rightmire, 2004, 2007, 2008 |
| Frontal keel | Narrow, high; separate from bregmatic eminence | Broad, low continuous with bregmatic eminence | Narrow, high; separate from bregmatic eminence | Broad, low; separate from bregmatic eminence | Santa Luca, 1980 |
| Most prominent aspect of midsagittal profile | Lower half of frontal squama | Upper half of frontal squama? | Lower half of frontal squama | ? | |
| Reduced postorbital constriction | Yes | Yes | No | No | |
| Relatively short, arched parietal | Yes | Yes | No (short, flat) | No (short, flat) | Weidenreich, 1943; 1951; Santa Luca, 1980 |
| Bossing of parietal walls relative to bimastoid width | Yes | Yes | No | No | |
| Obelion depression | No | Yes (variable) | Yes | Yes | Santa Luca, 1980 |
| Temporal squama contour | High, arched | High, arched | Low, flat or weakly arched | Low, flat or weakly arched | Santa Luca, 1980 |
| Articular tubercle stands out in some relief against flat preglenoid surface | Yes (left side only) | Yes | No | No | Weidenreich, 1943; 1951; Santa Luca, 1980 |
| Sphenoid spine extends inferiorly without contributing directly to medial wall of mandibular fossa | ? | Variable | Yes | Yes | Stringer, 1984; Martínez and Arsuaga, 1997 |
| Tympanic plate thickness | Slightly thicker than modern humans, thinner than *H. erectus* | Thin | Thick | Thick | Weidenreich, 1951; Martínez and Arsuaga, 1997 |
| Postglenoid process size/ projection | Medium | Medium | Small | Absent | Martínez and Arsuaga, 1997 |
| Length of occipital (lambda-inion) plane compared to nuchal (inion-opisthion) plane | Longer occipital vs. nuchal plane | Longer occipital vs. nuchal plane | Shorter or equal occipital vs. nuchal plane | Shorter occipital vs. nuchal plane | Weidenreich, 1943; Santa Luca, 1980 |
| Occipital angle | Moderately angled | Moderately angled (except Cepano) | Sharply angled | Sharply angled | |
| Inion separate from opisthocranion | Yes | Yes (exception: Ceprano) | No (exceptions: ZKD 10, 12) | No | |
| Anterior nasal sill is crested, may possess a prominent central spine | No | Yes | No | ? | |
| Nasiofrontal angle > 140° | Yes | Variable | Yes (based on reconstruction) | ? | Rightmire, 1998 |

TABLE 2. (Continued)

| Character | Dali | Afro/European MP Homo | Chinese H. erectus | Ngandong H. erectus | Additional references |
|---|---|---|---|---|---|
| Bulge between nasal aperture and orbits (paranasal inflation) | Yes | Variable | No | ? | Pope, 1992 |
| Maxillary body facies orientation | Posteroinferior | Anteroinferior | ? | ? | Maddux, 2011 |
| Maxillary process orientation | Slightly anteroinferior | Posteroinferior | ? | ? | |
| Maxillary sulcus present | Yes | No (Variable) | Yes | ? | Weidenreich, 1943 |

or less rectangular in shape with a slight curve along the squamosal margin. The sagittal margin exhibits slight keeling along the anterior portion. The sagittal suture itself is complex with numerous convolutions.

The parietal bones are relatively thick (Supporting Information SI Table 5 ). The area for the temporal muscle (*planum temporale*) is not flat, but expands posteriorly. In posterior view, the walls of the parietal bones are almost vertical along roughly the inferior one-third, and slightly convergent towards the superior two-thirds of the bone. Dali exhibits a bossing of the bones (parietal tubers) relative to the bimastoid width. The maximum bossing is located above the squamous temporal and just below the inferior curvature of the temporal lines. However, the maximum width of the cranium is not located on the parietals but further down on the temporal bone. The maximum biparietal breadth is 149.5 mm. No parietal foramen is visible nor is there a depression in the obelion region.

The craniometric landmark lambda is not preserved due to a broken extrasutural bone in a damaged portion of the posterior parietal bone. Thus, it is difficult to measure the absolute length of the parietal bone. Two positions are possible for lambda, the first estimated by extending the upper border of the extrasutural bone, the second by following the trend of the preserved part of the lambdoid suture and extending it up to the where it would intersect with the posterior projection of the sagittal suture (Fig. 4). For this study, we employed the latter method and obtained a parietal sagittal chord value of 107.0 and a parietal arc value of 115.0 mm. This yields a parietal index of 93. This, along with the bregma-asterion chord/biasterion breadth index (BAC/ASB $\times$ 100) of 113.9, is consistent with the observation that Dali's parietals are short but fairly arched.

### Temporal and mastoid regions

The temporal bones are relatively complete although the zygomatic process is broken on the left side, and the posterior squamous portion is missing on the right. The temporal squama of Dali is high and its superior border is arched. The height of the preserved left temporal squama is 46.5 mm and its length is 72.0 mm. The temporal squama angle following Martínez and Arsuaga's (1997) definition is 65°. The supramastoid crest forms the posterior part of the lower border of the squamous portion and continues above the external auditory porous to form the root of the zygomatic. The descending portion of the anterior squamosal border and the root of

the zygomatic process (which roughly forms the middle portion of the inferior border of the temporal squama) are joined by the anterior portion of the inferior squama border. Anterior to this the infratemporal crest is rounded rather than crest-like. The medial and lateral pterygoid plates are partially preserved on both sides.

The anterior portion of the temporal fossa is formed by the greater wing of the sphenoid, and it is deep but anteroposteriorly narrow, situated behind the processes of the frontal and zygomatic bones that make up the lateral orbit. At pterion, the parietal and sphenoid do not articulate directly with each other; each interfaces with a process extending from the superoanterior corner of the temporal squama. This process also connects with the frontal bone superoanteriorly. On the left side there is a rather robust temporal line that begins as the posterior margin of the supraorbital trigone and then divides into inferior and superior lines. After passing across the parietal boss the inferior line curves inferiorly, then antero-inferiorly, terminating at the supramastoid crest. The superior temporal line is less prominent, beginning about 30.0 mm behind the anterior margin of the browridge. The posterior portion of the superior temporal line turns inferiorly, then antero-inferiorly and terminates at the angular torus, which is more or less elliptical in shape. The right temporal lines are more or less similar, but the posterior parts are lost. On the left side the sutures between the parietal, occipital and temporal bones form the posterior and lower margins of the angular torus. Irregular foveae form the anterior margin and serve to demarcate the torus from the rest of the parietal bone. There is no demarcation between the upper part of the torus and the rest of the parietal. Dali possesses a parietal notch, the deepest point of which is approximately 25 mm anterior to asterion.

The zygomatic process of the temporal is preserved on the right side. The superior surface of the root is broad and roughly triangular in shape. There is a small tubercle with a broad base on the lateral margin of the zygomatic process about 24 mm anterior to auriculare. The outer margin is formed by a continuation of the supramastoid crest. Below this, the form of the external auditory meatus is elliptical and the longest axis is vertically oriented.

The maximum cranial width is located at the level of the supramastoid crest, which is a robust eminence with a broad base at its middle portion instead of a ridge. It is continuous with the root of the zygomatic process, which runs posteriorly and slightly superiorly. This crest crosses the squamosal suture and becomes continuous

with the inferior segment of the temporal line. A wide groove, the supramastoid sulcus, separates the supramastoid crest and the lateral surface of the mastoid process.

The mastoid region is characterized by processes that are not strongly projecting below the level of the cranial base, but are fairly broad with rugose markings. No mastoid foramen is visible. A mastoid crest appears on the superoanterior part of the lateral surface of the mastoid process. It is roughly rhomboid in shape with the long axis extending inferoanteriorly to superoposteriorly. The crest is separated from the supramastoid crest by a groove, which is broad anteriorly and narrow posteriorly. There is no anterior mastoid tubercle.

The processes are rimmed by a deep digastric groove medially, which lacks a raised ridge of bone along the anterior portion of the floor. On the left side, the groove has a narrow crest 14.0 mm in length and 4.0 mm in breadth, forming the paramastoid process. The paramastoid process is defined here as a structure parallel to the mastoid process, separated from it by the digastric groove (Caspari, 1991). Medial to the paramastoid process is a relatively shallow occipital groove bounded medially by a sharp ridge, the occipitomastoid crest, which is approximately 7 mm wide and located on the occipitomastoid suture itself. Together, the paramastoid process and the occipitomastoid crest make up the juxtamastoid eminence, following Rouvière (1954; Caspari, 1991). The crest is highest anteriorly and gradually reduces toward the posterior end where it joins a broader, quadrangular shaped elevation that connects with the attenuated extension of the occipital torus.

The tympanic plate forms the posterior wall of the glenoid fossa, which is deep and broad in the medio-lateral direction. The glenoid fossa does not have a horizontal floor. A trace of the stylomastoid foramen is evident anteromedial to the mastoid process. The styloid processes are absent, but a trace of the base is discernible on each side. The postglenoid processes on Dali are prominent but small, protruding downward from the zygomatic process of the temporal bone. Following the definition of Martínez and Arsuaga (1997), the postglenoid process length measures 18.0 mm. The transverse dimension of the basal (upper) section connecting with the zygoma is 5.0 mm. The articular eminence does not stand out in relief against the preglenoid surface: it is flat on the right side and relatively flat on the left.

The specimen displays some thinning of the tympanic plate, particularly relative to earlier *Homo* (Weidenreich, 1951; Martínez and Arsuaga, 1997).The tympanic plate is mediolaterally located. Several methods have been used to describe this region. Following Weidenreich's (1943) definition of tympanic plate orientation in ZKD, Dali's sit at an acute 79° angle relative to the midsagittal line. Based on Martínez and Arsuaga's (1997) assessment of this region, Dali's tympanic plate is coronally versus sagittally oriented. And following Terhune et al.'s (2007; Terhune, personal communication) definition, the vertical axis of Dali's tympanic plate is not anteriorly angled; rather it runs in the superoinferior direction. It is unclear if the sphenoid spine makes a contribution to the medial mandibular fossa.

## Occipital and cranial base regions

Dali's occipital bone is partially damaged, and the superior portion near the right lambdoid suture is missing. It is well preserved on the left side. Asterion is still bilaterally visible, based on the fact that the lateral portion of the occipital along the lambdoid suture is intact on the right side, as well as the posterior part of the temporal along the parietomastoid suture. As previously noted, Dali has an extrasutural bone in the position of lambda, making the identification of that landmark ambiguous. The basilar portion of the occipital is nearly complete, with a small part of the right anterior margin of foramen magnum missing. The occipital condyle is missing on the right side and is heavily worn on the left. The occipital bone is moderate in size with the occipital chord/arc index of 68.3 or 71.1 (based on two estimates of lambda) indicating that Dali has a relatively short occipital chord length relative to the arc length. The maximum breadth of the occipital bone is at asterion, with the biasterion breadth measuring 115.0 mm. It is not possible to tell if there is lambdoidal flattening.

In overall morphology, the occipital bone exhibits flexion between the upper occipital and lower nuchal planes. The occipital angle (Howells 1973) is 96°. The profile of the occipital plane is relatively vertical. Dali possesses an occipital torus at the juncture between the occipital and nuchal planes, making the transition angular but possessing a relatively smooth contour. Here, the term "occipital plane" is referring to the upper scale of the occipital bone, from lambda to the superior nuchal lines, while the term "nuchal plane" refers to the lower scale from the nuchal lines to the cranial base. The torus extends across the majority of the width of the occipital, is rhomboid in shape, and measures about 90 mm transversely and about 30 mm in height. Above the torus is a very shallow supratoral groove but there is no suprainiac fossa. The superior nuchal line is composed of a medial and lateral section. The medial section is slightly thicker than the lateral portion, and no linear tubercle is present below it. The medial section of the superior nuchal lines acts as the antero-inferior limit of the occipital torus. The lateral section of the superior nuchal line is a narrow ridge, acting as the lateral elongation of the occipital torus and forming the postero-lateral border of the nuchal plane.

The superior nuchal lines join at inion. Since there is no linear tubercle proper (Hublin, 1978; Rightmire, 1990; Caspari, 1991) or external occipital protuberance, inion is defined here following Martin and Saller (1957) as the point at which the superior nuchal lines unite with the median sagittal plane. Inion is 22.0 mm anterior and inferior to opisthocranion and is located at the junction between the occipital and nuchal planes while opisthocranion is located on the occipital plane. Inion and endinion are separated by 11.0 mm. The inferior nuchal lines form a palpable ridge about 30 mm from the superior nuchal lines, but are not very well developed. There is no external occipital crest, but instead a broader eminence between shallow depressions on either side for the attachment of the semispinalis capitis muscles. The upper plane of Dali's occipital bone is long in comparison with the nuchal plane, with the former (lambda-inion chord) measuring 84.0 mm or 74.0 mm, respectively, from the higher and lower positions of lambda (i.e., at the superior vs. inferior border of the central part of Wormian bone). The lower scale from inion to opisthion measures 39.0 mm, giving Dali an occipital scale index (IOC/LIC × 100) of 46.4 or 52.7 from the two estimates of lambda, respectively.

## Facial skeleton

Dali has a relatively broad face with large orbits and a broad nasal aperture. The malar region is vertically short relative to other Middle Pleistocene hominins such as Petralona and Broken Hill, but is noticeably laterally projecting. The maxilla is damaged on both sides where it exhibits a superior displacement of the palate. This has led to damage to the left infraorbital region as well. On the right side the palate is slightly displaced posteriorly but the infraorbital and zygomatic portions are intact as is the frontal process of the maxilla.

There have been questions regarding the extent to which the facial height of Dali has been artificially reduced by postdepositional deformation (Stringer, 1990). While the palate has been considerably damaged, the facial height—particularly vertical displacement of the maxilla—is minimal, an assessment also reflected in Pope (1992). While a correction of this distortion would no doubt slightly increase the facial height values for Dali, it would not do so considerably. So while a full CT-guided reconstruction of Dali is necessary for a more accurate assessment of its facial dimensions, the distortion is minimal enough to allow for an assessment of Dali's facial morphology in a comparative context.

The orbits are roughly square, although the lateral wall is slightly longer than the medial wall. The form of orbit appears similar to the Steinheim specimen, although it is unclear if postmortem deformation has affected this region in Steinheim. The inferolateral orbital rim is rounded and the floor of the orbit is depressed relative to this margin, falling into Lahr's (1996) RO2 category, which is the most common condition in modern humans. The orbital roof possesses clear lacrimal fossae, and this region extends to the articulation with the lesser wing of the sphenoid. The orbital index (OBH/OBB $\times$ 100) is 75.6 and the interorbital width (Howell's DKB) is 26.0 mm.

The nasal bones are very narrow, measuring 7.0 mm wide together at the midpoint. The frontonasal and frontomaxillary sutures form a slightly curved line. The nasal aperture is broad and does not appear to be very tall, exhibiting a roughly equilateral triangular shape with a slight convexity toward the lateral sides. However, the inferior margin of the nasal region has been slightly superiorly displaced due to distortion. A CT-guided reconstruction could shed light on the actual nasal height, as well as the configuration of the nasal cavity floor, which has not been cleared. The nasiofrontal (NFA) angle is 143°, which is characteristic of a less projecting nasal region relative to the upper face (Franciscus and Trinkaus, 1988). There is a slight bulge between the pyriform aperture and the orbits, a paranasal inflation also noted by Pope (1992).

On the right side, the infraorbital region itself is relatively gracile. Following previous descriptions of the infraorbital region (Arsuaga et al., 1999; Maddux, 2011), Dali possesses a posteroinferiorly oriented maxillary body facies and slightly anteroinferiorly oriented maxillary process, which differentiates it from the African and European Middle Pleistocene specimens. A large infraorbital foramen is visible on the right maxilla, positioned about 20 mm from the nasal aperture and 7.5 mm below the inferior orbital rim. In contrast to Rightmire's (2004) description, we do find the presence of a maxillary sulcus—on Dali this takes the form of a groove or furrow extending from about 5 mm from the base of the infraorbital foramen to the superior alveolar border, conforming to Weidenreich's (1943) description of a sulcus maxillaris. This groove is approximately 12 mm long, and does not excavate the infraorbital surface to the extent necessary to be considered a canine fossa (Maureille, 1994; Rightmire, 1998a, 2006; Maddux, 2011). About 7.5 mm lateral to the infraorbital foramen is a rounded depression; however, this depression is too laterally positioned to be referred to as a canine fossa as traditionally defined (Maureille, 1994; White and Folkens, 2000).

The position of the zygomatic root is possibly affected by the postdepositional damage to the palate, but is at P4 or M1. The zygomaticoalveolar margin is nearly horizontal in orientation, with an inferior edge that is rounded rather than crest-like (Pope, 1991). A distinct malar tubercle, following the definition of Pope (1991), is situated lateral to a shallow malar notch. The position of the zygomaticomaxillary suture is oblique, and no infraorbital suture can be seen on the specimen. The lateral nasal margin appears to be non-everted following Maddux and Franciscus (2009).

Stringer (1984) defined *H. erectus* as having a short broad face, which was determined by having an upper facial height (NPH/FMB $\times$ 100) index of less than 70. By necessity this baseline could not take the ZKD *H. erectus* sample into consideration since none of the specimens has preserved the morphology for frontomalare breadth (FMB) or nasion-prosthion height (NPH) measurements. We therefore calculated Dali's upper facial index using NPH versus bizygomatic breadth (ZYB) and compared the value with a sample of Middle and Late Pleistocene specimens as well as modern Chinese (Supporting Information SI Table 6). Based on this modified estimate of the upper facial index, Dali's value (51.7) indicates a relatively short, broad face as has previously been described for it.

## Cranial capacity and encephalization

The estimated cranial capacity for Dali is 1,120 cm³ (obtained using millet seed) placing it within the range of the Zhoukoudian specimens (1,029 $\pm$ 126.4 cm³, $n = 7$) and the Ngandong sample (1,151 $\pm$ 99.5 cm³, $n = 5$) sample. It is also within the range of the Afro/European sample (1,189 $\pm$ 107.2 cm³, $n = 9$), but above the value of the Hexian specimen (1,025 cm³) and considerably below the estimated cranial capacity for Jinniushan (1390 cc) (Weidenreich, 1943; Qiu et al., 1973; Wu and Dong, 1982; Wu and Poirier, 1995; Holloway et al., 2004).

The estimated encephalization quotient (EQ) for Dali is 5.3 (Rightmire, 2004), calculated using orbit size as a proxy for body mass (Aiello and Wood, 1994; Kappelman, 1996). This is also the mean value for the other MP Afro/European hominins in Rightmire's (2004) study (5.3 $\pm$ 1.29) and while this is an imperfect measure, it demonstrates that Dali possibly possesses considerable encephalization over the Zhoukoudian sample (XI and XII) whose average estimated EQ is 4.6, although a one-tailed *t*-test between Dali/Jinniushan versus the ZKD sample was marginally above significance ($P = 0.07$). Dali is different from the ZKD sample in having both an absolutely larger brain size and smaller estimated body mass. Overall, Dali conforms to the pattern of increased encephalization described by Rightmire (2004, 2008) among the Afro/European mid-Pleistocene sample, distinguishing it from *H. erectus* in this respect.

## SIMILARITIES BETWEEN DALI AND ASIAN *HOMO ERECTUS*

### Cranial vault and base

Several researchers have noted affinities between H. *erectus* and Dali in features such as supraorbital torus thickness and development, frontal keeling, parietal bone thickness, a relatively low cranial vault, and the presence of extrasutural bones and an angular torus (Kennedy, 1990; Pope, 1992; Rightmire, 1998b; Etler, 2004). While these traits are present on Dali, the question of whether they are strictly characteristic of *H. erectus* merits some consideration. In addition, certain traits seem to align Dali not necessarily with Asian *H. erectus* in particular, but with the Chinese archaic sample in general.

First, Dali's parietal bone thickness (11.2 mm, taken on parietal eminence) is in the upper range of the Afro/European MP sample (average is $10.5 \pm 1.2$ mm, $n = 4$), exceeded only by Swanscombe (12 mm) and Ceprano (16 mm) (Kennedy, 1990; Ascenzi et al., 2000). It falls well within the range of the ZKD *H. erectus* sample ($11.78 \pm 2.3$ mm, $n = 6$) (Weidenreich, 1943) (Supporting Information SI Table 5). However, while thick cranial bones are characteristic of Asian *H. erectus* (Andrews, 1984; Gauld, 1996), they are not unique to them and are present elsewhere in the Old World during the Middle and Late Pleistocene (Stringer, 1984; Kennedy, 1990) and thus Dali's affinity on this matter is neither exclusive to one group nor diagnostic.

Second, the extrasutural bone present on Dali is a common feature in Asian *H. erectus* but is also not unique to this group. These are also found on European Middle Pleistocene specimens such as Vérteszöllös, Petralona, and certain individuals from the Sima de los Huesos (SH) site at Atapuerca, for example (Wolpoff, 1971; Stringer et al., 1979; Manzi et al., 2000). Similarly, the presence of an angular torus on Dali aligns it with *H. erectus* from China (found on the ZKD specimens, Nanjing, and Hexian) but not uniquely so. Andrews (1984) considered this an Asian *H. erectus* autapomorphy, although Rightmire (1985, 1996) questioned its utility noting that it was not necessarily unique to the region or even to *H. erectus*. An angular torus is also found on the later Middle Pleistocene specimen from Jinniushan and the *H. sapiens* fossils from Ziyang and Chuandong and has been noted on several Afro/European Middle Pleistocene specimens including Arago 21, Petralona, SH 4 and 5, Bodo, and Broken Hill, as well as the Indian Narmada specimen (Stringer et al., 1979; Asfaw, 1983; Kennedy et al., 1991; Arsuaga et al., 1997), and several anatomically modern Australians including WLH 50 and Kow Swamp (Frayer et al., 1993; Curnoe, 2007).

In addition, while the coincident position of inion and opisthocranion points is considered distinctive of *H. erectus*, the Zhoukoudian sample show some variability on this: on Skulls X and XII the two points are separated by approximately 12 mm. Similarly, there is some debate as to whether small versus developed postglenoid processes are characteristic of Asian Middle versus Late Pleistocene *Homo* (Weidenreich, 1943; Santa Luca, 1980; Pope, 1992; Etler, 1994; Martínez and Arsuaga, 1997). Early modern humans and Neandertals have been shown to exhibit relatively projecting postglenoid processes (Martínez and Arsuaga, 1997). As with parietal thickness, the presence of Wormian bones and an angular torus, the separation of inion and endinion, and the presence of prominent but small postglenoid processes on Dali are consistent with Chinese *H. erectus* morphology in some respects but do not uniquely align it to this group.

Finally, on Dali the vertical axis of the tympanic plate is not anteriorly angled as has been described for Asian *H. erectus* (Weidenreich, 1943; Terhune et al., 2007). Rather, it runs superoinferiorly as does the vertical axis of the external auditory meatus, without anterior angulation. Following Weidenreich's (1943; p. 202) description of this region in the Zhoukoudian specimens, the tympanic plate of Dali is more frontally oriented than the ZKD *H. erectus*, whose plate lies parallel to the basal surface of the skull and is more horizontally oriented. In this respect, Dali's tympanic plate orientation is more derived than that of Asian *H. erectus*. Martínez and Arsuaga (1997; p. 289) state: "There is a wide consensus that the axis of the tympanic plate is coronally oriented in *H. erectus* (i.e., near perpendicular to the sagittal plane) and that it is sagittally oriented in modern humans" (see references therein). They find that the sagittal orientation is common in African MP *Homo* while the coronal orientation is common among the SH sample as well as Neanderthals, and describe Dali as possessing this morphology. However, following their definition of this trait, an examination of the original specimen reveals that Dali's tympanic plate is coronally oriented, thus aligning it with the *H. erectus*, SH, and Neanderthal samples. Thus, depending on the specific aspect of tympanic morphology being examined, Dali's configuration in several regions aligns it with Asian *H. erectus* in some respects, and differentiates it from this sample in others.

However, there are certain features distinctly shared between Dali and Chinese Middle Pleistocene specimens. First, while in most respects Dali's supraorbital torus is similar to Afro/European MP *Homo*, the form of the supraorbital arches and frontal keel align it primarily with the Chinese ZKD, Hexian, and Maba specimens who share a similar (but weaker) narrow based keel with a relatively high ridge. This is in contrast to the Afro/European sample where the keel is more broad-based, situated towards the posterior portion of the frontal, and is continuous with the bregmatic eminence. Second, Dali's long, low cranium (Supporting Information SI Table 3 ) is also comparable to that of the Zhoukoudian sample and falls below that of the Afro/European Middle Pleistocene sample. Third, as stated earlier, the position of the most prominent aspect of the midsagittal profile is on the lower half of the frontal squama, aligning Dali with other Middle and Late Pleistocene Chinese. Fourth, in the temporo-mandibular region, the articular eminence on Dali does not stand out in relief against the preglenoid surface, in contrast to what has been described for some African and European mid-Pleistocene hominins as well as *H. erectus* (Martínez and Arsuaga, 1997; Antón, 2003; Rightmire, 2004). Finally, in the occipital region, the transition between the occipital and nuchal planes on Dali is angular instead of rounded, a condition similar to *H. erectus*, which according to Stringer (1984) is characterized by a highly angled (OCA $\leq 107°$) occipital.

### Facial skeleton

Like many aspects of the neurocranial vault, Dali's facial skeleton has a number of traits that distinctly align it with the Pleistocene Chinese sample. For example, as

Supporting Information (SI) Table 6 shows, Dali falls within the range of the archaic and anatomically modern *H. sapiens* from China and well below the range of the Afro/European MP sample. The specimens from Bodo, Broken Hill, Petralona, and Sima de los Huesos all have indices above 55.0. In contrast, all Chinese specimens have values below 55.0. Each of the Chinese samples is significantly different from the Afro/European MP sample ($p < 0.001$, one-tailed *t*-test). It is worth noting that while the MP Chinese sample is significantly different from the modern Chinese males and females ($p = 0.05$, $p = 0.01$, respectively), the Late Pleistocene Chinese are not significantly different from either the MP Chinese ($p = 0.14$) or the modern Chinese males or females ($p = 0.90$, $p = 0.28$, respectively), suggesting some continuity in this feature within this region. According to Rightmire (2008), upper facial height in particular has a low coefficient of variation (CV) among Afro/European Middle Pleistocene *Homo* and as such may carry more taxonomic valence than other measurements. Dali's upper facial height alone is considerably shorter than Petralona, Broken Hill, Bodo, and SH 5. Even with correction of the distortion, it is unlikely that Dali's value would meet or exceed that of these specimens, which are all 10 mm greater than Dali. The entire Chinese *H. erectus* sample has a mean value of 76.6 ($\pm 4.5$) mm based on Nanjing 1 as well as the two ZKD reconstructions. These values suggest continuity within China with regards to the presence of a relatively short, broad face.

Both the interorbital (DKB) and biorbital (EKB) breadth values for Dali are comparatively low (26.0 mm and 110.0 mm, respectively), falling outside the range of the Afro/European specimens and well within the range of the Asian samples. The values for the Afro/Europeans are driven by the large breadths of Bodo, Broken Hill, and Petralona, which are more than 10 mm greater than Dali in both dimensions. This further suggests that Dali's upper facial index value is driven more by a short face than an excessively broad one, a trait that seems to be a general archaic Asian one.

In the infraorbital region, the orientation of Dali's maxillary body facies and maxillary process align Dali most closely with the Chinese *H. erectus* (namely, reconstructions of the ZKD specimens as well as Nanjing 1) and with modern *H. sapiens* (Maddux, 2011). The presence of a sulcus maxillaris was noted by Weidenreich on the ZKD fossils (Weidenreich, 1943), and it is also present on the Nanjing 1 specimen. It has been described on WT-15000 as well (Arsuaga et al., 1999), however, and Rightmire (2004) thus considers it an ancestral trait. Interestingly, though, it is absent in later *Homo*, including most Afro/European Middle Pleistocene hominins. The nearly horizontal orientation of the zygomaticomaxillary crest and more laterally situated malar tubercle is also found on Chinese *H. erectus* as well modern *H. sapiens*, and is likely a secondary consequence of the overall smaller face shared among these groups (Maddux, 2012). Importantly, this region was not affected by postdepositional factors and thus refutes the notion that the midface of Dali would be considerably more robust after a correction of the distortion.

## DALI COMPARED TO AFRICAN AND EUROPEAN MIDDLE PLEISTOCENE *HOMO*
### Neurocranium

According to Rightmire (2004, 2008), who has offered the most detailed assessment of the distinguishing traits

by which to define the taxon *H. heidelbergensis*, the African and European specimens are characterized by a series of traits outlined in Table 2. These include aspects of the cranium that are related to increased globularity, presumably due to larger brain size, and certain aspects of the upper and midfacial regions. Overall, as Rightmire (2008) notes, the form of these specimens is *H. erectus*-like but with some structural distinctions.

Several aspects of Dali's morphology align it with the Afro/European MP sample. Many of these are related to the overall expansion of the neurocranium; however, in the facial skeleton as well, Dali exhibits some affinities with this group. The thickest part of Dali's supraorbital torus is in the central portion above each orbit, which is nearly identical to the conditions seen on Ceprano, Petralona, and Broken Hill and is thicker than the Ngandong and Zhoukoudian samples. Dali also shares with the Afro/European specimens a weaker supratoral sulcus than is present on *H. erectus*, which SA believes could be the result of increased encephalization, although the supratoral sulcus on the Ceprano is more archaic in form than Dali's, with the browridge receding directly into a low frontal squama (Ascenzi et al., 1996). The more archaic form of the torus and squama is consistent with the notion that Ceprano could represent an ancestral stock of the *H. heidelbergensis* lineage (Manzi, 2011). Like other members of the Afro/European MP sample, Dali exhibits increased projection of the lateral brow (Athreya, 2009), which is a distinctive trait for this group. At glabella, Dali's projection is most similar to the African specimens from Bodo, Florisbad, and Elandsfontein. It has a more projecting glabellar region than the Broken Hill or Ceprano specimens, the latter of which has a glabellar sulcus. At the midbrow, Dali's supraorbital torus projection is nearly identical to Bodo and in the lateral aspect it overlaps with the prominently projecting tori of specimens from Petralona and Broken Hill. This is in contrast to the Asian *H. erectus* sample, where the browridge is roughly equally projecting in the midline and lateral portions.

The frontal bone of Dali overall shows broadening relative to the *H. erectus* sample. The ratio of minimum to maximum frontal breadth on Dali is 88.2 (Supporting Information SI Table 3 ) far above the Chinese *H. erectus* average of 80.8 ($\pm 2.5$, $n = 4$). In absolute terms as well, the 119.0 mm XFB and 105.0 WFB values for Dali are in line with the later Pleistocene and modern human sample means and well above the 110.3 mm (XFB) and 87.4 (WFB) mean values for Chinese *H. erectus* ($\pm 4.3$ and 4.8, $n = 6$ and 7, respectively). Dali has less postorbital constriction than the Bodo and Ceprano and Broken Hill specimens. Its index of 85.9 is less than the Sima de los Huesos specimens, however, falling very close to that of Petralona, which has a PO constriction index of 87.3 using Kimbel et al.'s (1984) definition defined above. In general, Dali exhibits reduced postorbital constriction and a movement away from the *H. erectus* condition.

There is bossing of the parietal walls relative to the bimastoid width on Dali, similar to the Afro/European MP condition (Rightmire, 2008). The parietal walls are more vertical when viewed from behind than is observed in *H. erectus* where the walls converge immediately above the position of maximum cranial breadth, which is usually at the supramastoid crest (Stringer, 1984). Middle Pleistocene *Homo* has been described as having parietal walls that are slightly convergent toward the top, and occasionally parallel (Rightmire 2004), a condition

present on Dali. The short, arched shape of the parietals on Dali is derived as well, based on the BAC/ASB index. Dali's index value of 113.9 is close to that of other Middle Pleistocene hominins such as SH 5 (111.3) (Arsuaga et al., 1997), Petralona (109 or 116) and Broken Hill (113) (Stringer, 1983) and is well above the average value of around 100 for Asian *H. erectus* (Arsuaga et al., 1997).

The presence of a depression at obelion was considered by Weidenreich (1937) to be an ancestral trait among Chinese and Indonesian *H. erectus*. Thus, Dali's absence of a depression here is derived relative to the archaic Chinese *H. erectus* condition. However, a few MP hominins from Sima de los Huesos, Swanscombe, and Broken Hill possess a depression at obelion as do a few early *H. sapiens* (Omo 1, Eliye Springs), so there is not a strict correspondence between the presence of this trait and age or taxonomic affiliation.

Dali's temporal squama is aligned with the derived condition described recently in a comprehensive morphometric study of temporal squama morphology in the genus *Homo* (Terhune and Deane, 2008). These authors found that Neandertals and *H. erectus* share low, less arched squamae while *H. heidelbergensis* and *H. sapiens* have higher, more arched temporal squamae. Rightmire (2007) noted that what is particularly diagnostic in this region of the skull among Afro/European Middle Pleistocene *Homo* is the absolute height of the temporal squama, and in this respect Dali's value (46.5 mm) is high relative to Chinese *H. erectus* with the average height for the ZKD sample being 36.0 mm ($\pm$1.9, $n = 5$) (Weidenreich, 1943).

Also on the temporal, a comparatively delicate tympanic plate is a trait that may distinguish *H. heidelbergensis;* studies support the thinning of the tympanic plate as a derived feature typical of *H. sapiens* (Kennedy, 1990). Dali exhibits an intermediate but more derived condition in that while it has a relatively thick tympanic plate compared to modern humans, it is thinner than that of *H. erectus* as well as earlier *Homo*. Weidenreich (1943) described the ZKD specimens as having a raised ridge of bone along the anterior portion of the floor of the digastric groove, and the same trait is considered a Neandertal autapomorphy (Vallois, 1969; Stringer, 1984; Martínez and Arsuaga, 1997). However, this trait is absent in most other members of the genus *Homo*, and Dali lacks this trait thus aligning it with the Afro/European Middle Pleistocene *Homo* sample. Dali's occipital bone is similar to the specimens from Petralona and Broken Hill in being relatively broad and low. Like these two specimens, the upper (occipital) plane is vertical when viewed in *norma lateralis* unlike the anteriorly sloping upper occipital plane of Chinese *H. erectus*. Dali's estimated occipital angle of 93° is comparable to Petralona (97°). The latter has a highly angled occipital, falling within the range of Indonesian *H. erectus* (95°–102°). Ceprano has also been described as having a highly angled occipital as well (Ascenzi et al., 1996). It clearly has a more primitive posterior cranium with a shorter occipital plane, stronger torus, and a coincident position of opisthocranion and inion, representing a more archaic form both morphologically and possibly phylogenetically (Ascenzi et al., 2000; Manzi et al., 2001; Manzi, 2004). Dali aligns with Afro/European MP *Homo* in having a smaller separation of inion and endinion (<25 mm), although the utility of this trait in distinguishing *H. erectus* (from later forms of the genus *Homo* is questionable (Balzeau et al., 2011).

## Facial skeleton

Dali's midface shows some affinities to the Afro/European MP *Homo* sample, although it is more like the *H. erectus* sample in most respects. However, the bulge between the pyriform aperture and the orbit on Dali is also found in African (Broken Hill, Bodo) and European (Petralona, Arago) Middle Pleistocene *Homo*. In contrast, other Pleistocene human crania of China have no bulge in this region. The breadth of Dali's pyriform aperture falls at the high end of the archaic sample in general. The highest values are seen among the Afro/European MP and Neandertal samples, and Dali's values are in line with these and above the mean for the *H. erectus* and Asian MP samples. A larger nasal breadth is correlated with higher precipitation or humidity levels (Franciscus and Long, 1991). The nasal height for Dali, however, is relatively low—below that of the other archaic *Homo* samples—however, the lower margin of the pyriform aperture was slightly superiorly displaced by postmortem deformation. Present measurements of Dali's nasal aperture yield a relatively high nasal index (62.3), suggesting adaptation to a relatively warmer, moister environment. The possible position of the zygomatic root at P4/M1 would align Dali with other Eurasian and African Middle Pleistocene hominins including Asian *H. erectus* (Trinkaus, 1987; Rightmire, 1998a) and thus does not appear to be diagnostic.

## DISCUSSION

Overall Dali shares several traits with the Afro/European MP group. The frontal, parietal, and temporal bones exhibit evidence of overall cranial expansion. The parietals, though short, are more arched and slightly more horizontally-oriented superiorly and exhibit bossing relative to the bimastoid width. The temporal squama is likewise high with an arched superior margin contour, as opposed to being flat. The occipital does show an increased length of the occipital plane in comparison to the nuchal plane. The more derived nature of the occipital bone is also evident in the separation of inion and opisthocranion. All of these are likely related to Dali's brain expansion, and its encephalization follows on the trend observed among other MP *Homo,* who have a higher EQ relative to *H. erectus* (Rightmire, 2004).

In a few respects, though, Dali fails to conform to the general pattern exhibited by the African and European MP samples. Its notably low cranial height and more angulated occipital are different than that described by Rightmire (2004, 2007, 2008) for *H. heidelbergensis*. It also lacks the raised typical preglenoid morphology, conforming more to the ZKD *H. erectus* condition of having a planum preglenoidale vs. a raised articular surface. In other traits not listed by Rightmire as being diagnostic of Afro/European MP *Homo*, Dali is also aligned either with Chinese *H. erectus* or other Chinese MP hominins such as Maba and Jinniushan. The absence of a supraorbital notch, short parietal profile, presence of a weak angular torus, relatively thick parietal bones and moderately thick tympanic plate are among these shared traits. In addition, and perhaps most distinctive, is Dali's short and relatively nonprognathic face. This is consistent with the pattern observed among other Middle and Late Pleistocene Chinese in contrast with those from Europe and Africa.

Without having a commonly agreed-upon benchmark to weight these character traits, an interpretation of their individual and collective significance is necessarily a subjective exercise. Additionally, it is unclear how many of them are correlated character complexes. However, this description of Dali confirms studies that have described it as "transitional" and have noted the presence of such forms in Middle Pleistocene China (Pope, 1992; Etler, 1996, 2004). For some, the presence of "transitional" morphology is sufficient to include a specimen in the *H. heidelbergensis* hypodigm (e.g., Campbell et al., 2006; Jurmain et al., 2010). However, just what that transition represents continues to be the subject of some debate and therein lays the problem, because while the prevailing paradigm in the field today is that *H. heidelbergensis* is a valid taxon, the details of its phylogenetic history and membership have yet to be determined (Athreya, 2007; Bräuer, 2008; Hublin, 2009; Rightmire, 2009; Stringer, 2012). While Dali shares many traits with other specimens typically assigned to this taxon, there is considerable debate as to whether that term should be restricted regionally or temporally to certain fossils from Europe and/or Africa (Arsuaga et al., 1997; Athreya, 2006; Rightmire, 2008).

We do not think that this single specimen can resolve these outstanding questions. Given the overlap that is inherent in such transitions—and the lack of uniformity that necessarily will exist among regions—we are reluctant to assign Dali to a particular taxonomic group on the basis of the morphology described here. Specifically, until more contemporaneous fossils from China are found, better direct dates for the existing evidence from China are provided, and a more clear understanding of the evolutionary history of *H. heidelbergensis* is achieved, it would be premature to place Dali in this group. At this stage, because of these limitations, any taxonomic designation we offer for Dali would be subject to debate.

The confounding factor is actually not Dali's mixed morphology, but the overlap that exists between *H. erectus* and non-*erectus* MP *Homo*—a fact that has been observed for some time (Wolpoff, 1980; Stringer, 1981; Athreya, 2003; Rightmire, 2008). This overlap reflects the fact that the evolutionary trajectory from archaic to more modern forms was the result of highly variable patterns of population dynamics across the Old World between different regional groups. Clearly China had a transition that cannot be subsumed under scenarios devised for Africa or Western Europe. What that means taxonomically would be premature to say. We therefore emphasize the patterns of morphological affinity that Dali exhibits, and the processes that could have shaped them.

In particular, Dali shares traits with Middle Pleistocene Europeans, Mid-to-Late Pleistocene Chinese, and in some cases, Africans of the Middle and early-Late Pleistocene. Wu (1988, 1990, 2004) has proposed the Continuity with Hybridization model that posits gene flow between eastern and western Eurasia, which is a possibility that merits further investigation (see Pope, 1991; Pearson, 2008; Liu and Wu, 2011). In this scenario, the suite of traits exhibited by Dali could be indicative of a local transition between *H. erectus* and *H. sapiens* that included some influence from western Eurasian populations during the Middle Pleistocene. This model is based both on the morphology described here as well as a more thorough multivariate analysis of Dali that is forthcoming (Athreya and Wu, in preparation). Importantly, it emphasizes the *processes* that contributed to the morphology observed in Dali regardless of its taxonomic allocation, which is arguably the more important point for paleoanthropologists.

## CONCLUSION

Assuming that the Dali specimen is typical of the population from which it was derived, the morphology it possesses suggests that the hominins of this region were undergoing a transition during the late Middle Pleistocene. The populations appear to be transitioning from the archaic morphology of Chinese *H. erectus* to the more derived morphology present in several European/African non-*erectus* as well as some Late Pleistocene Chinese specimens. Whether that transition represents an in situ evolutionary trend and/or the influence of population movements or gene flow from regions west (Africa/Europe/Central Asia) or southeast remains to be determined. A forthcoming study (Athreya and Wu, in preparation) explores in more detail the implications of Dali's morphology for the phylogeny and systematics of Middle Pleistocene *Homo*, particularly the *H. heidelbergensis* hypodigm. However, more specimens and more secure dates for the Chinese fossil record are ultimately needed in order to establish the source and trajectory of the phase of evolution represented by Dali in Middle Pleistocene China.

## ACKNOWLEDGMENTS

## LITERATURE CITED

Aiello LC, Wood BA. 1994. Cranial variables as predictors of hominine body mass. Am J Phys Anthropol 95:409–426.

Andrews P. 1984. An alternative interpretation of the characters used to define *Homo erectus*. Cour Forschungs Senck 69:167–175.

Antón SC. 2003. Natural history of *Homo erectus*. Yearb Phys Anthropol 46:126–170.

Arsuaga J-L, Martínez I, Gracia A, Lorenzo C. 1997. The Sima de los Huesos crania (Sierra de Atapuerca, Spain). A comparative study. J Hum Evol 33:219–281.

Arsuaga J-L, Martínez I, Lorenzo C, Gracia A. 1999. The human cranial remains from Gran Dolina Lower Pleistocene site (Sierra de Atapuerca, Spain). J Hum Evol 37:431–457.

Ascenzi A, Biddittu I, Cassoli PF, Segre AG, Segre-Naldini E. 1996. A calvarium of late *Homo erectus* from Ceprano, Italy. J Hum Evol 31:409–423.

Ascenzi A, Mallegni F, Manzi G, Segre AG, Segre Naldini E. 2000. A re-appraisal of Ceprano calvaria affinities with *Homo erectus*, after the new reconstruction. J Hum Evol 39:443–450.

Asfaw B. 1983. New hominid parietal from Bodo, Middle Awash Valley, Ethiopia. Am J Phys Anthropol 61:367–371.

Athreya S. 2003. A quantitative assessment of patterns of geographical variation in Middle Pleistocene *Homo* frontal bone morphology using Fourier analysis [Ph.D. Dissertation]. St. Louis, MO: Washington University.

Athreya S. 2006. Patterning of geographic variation in Middle Pleistocene *Homo* frontal bone morphology. J Hum Evol 50:627–643.

Athreya S. 2007. Was *Homo heidelbergensis* in South Asia? A test using the Narmada fossil from central India. In: Petraglia MD, Allchin B, editors. The evolution and diversity of humans in South Asia. New York: Springer Academic Publishers. p 137–170.

Athreya S. 2009. A comparative study of frontal bone morphology among Pleistocene hominin fossil groups. J Hum Evol 57:786–804.

Athreya S. 2010. South Asia as a geographic crossroad: patterns and predictions of hominin morphology in Pleistocene India. In: Norton C, Braun DR, editors. Asian paleoanthropology: From Africa to China and beyond. New York: Springer Netherlands. p 129–141.

Balzeau A, Grimaud-Hervé D, Gilissen E. 2011. Where are inion and endinion? Variations of the exo- and endocranial morphology of the occipital bone during hominin evolution. J Hum Evol 61:488–502.

Bräuer G. 2008. The origin of modern anatomy: by speciation or intraspecific evolution? Evol Anthropol 17:22–37.

Campbell BG, Loy J, Cruz-Uribe K. 2006. Humankind emerging. Boston: Pearson Allyn and Bacon.

Caspari RE. 1991. The evolution of the posterior cranial vault in the central European Upper Pleistocene [Dissertation]. Ann Arbor: University of Michigan.

Cunningham DJ. 1908. The evolution of the eyebrow region of the forehead, with special reference to the excessive supraorbital development in the Neanderthal race. Trans R Soc Edinb 46:283–310.

Curnoe D. 2007. Modern human origins in Australasia: testing the predictions of competing models. Homo 58:117–157.

Etler D. 2004. *Homo erectus* in East Asia: human ancestor or evolutionary dead-end? Athena Rev 4:37–50.

Etler DA. 1996. The fossil evidence for human evolution in Asia. Annu Rev Anthropol 25:275–301.

Franciscus RG, Long JC. 1991. Variation in human nasal height and breadth. Am J Phys Anthropol 85:419–427.

Franciscus RG, Trinkaus E. 1988. Nasal morphology and the emergence of *Homo erectus*. Am J Phys Anthropol 75:517–527.

Frayer DW, Wolpoff MH, Thorne AG, Smith FH, Pope GG. 1993. Theories of modern human origins: the paleontological test. Am Anthropol 95:14–50.

Gao X. 1999. A discussion of the "Chinese Middle Paleolithic". Acta Anthropol Sinica 18:1–16 (in Chinese with English abstract).

Gao X, Norton CJ. 2002. A critique of the Chinese 'Middle Palaeolithic'. Antiquity 76:397.

Gauld SC. 1996. Allometric patterns of cranial bone thickness in fossil hominids. Am J Phys Anthropol 100:411–426.

Heslop D, Langereis CG, Dekkers MJ. 2000. A new astronomical timescale for the loess deposits of northern China. Earth Planet Sci Lett 184:125–139.

Holloway RL, Broadfield DC, Yuan MS. 2004. The human fossil record, Vol. 3: Brain endocasts: the paleoneurological evidence. Hoboken, NJ: Wiley-Liss.

Hublin J-J. 1978. Le torus occipital transverse et les structures associées. Evolution dans le genre *Homo*. [3rd cycle Thesis]. Paris: University of Paris VI.

Hublin J-J. 2009. The origin of Neandertals. Proc Natl Acad Sci USA 106:16022–16027.

Hublin J-J. In press. The Middle Pleistocene record. On the ancestry of Neandertals, modern humans and others. In: Begun D, editor. A companion to paleoanthropology. Malden, MA: Wiley-Blackwell.

Indriati E, Swisher CC, III, Lepre C, Quinn RL, Suriyanto RA, Hascaryo AT, Grün R, Feibel CS, Pobiner BL, Aubert M, Lees W, Antón SC. 2011. The age of the 20 meter Solo River terrace, Java, Indonesia and the survival of *Homo erectus* in Asia. PLoS One 6:e21562.

Jin C, Kawamura Y, Taruno H. 1999. Pliocene and Early Pleistocene insectivore and rodent faunas from Dajushan, Qipan-shan and Haimao in north China and the reconstruction of the faunal succession from the Late Miocene to the Middle Pleistocene. J Geosci Osaka City Univ 42:1–19.

Jurmain R, Kilgore L, Trevathan W, Ciochon RL. 2010. Introduction to physical anthropology. Belmont, CA: Wadsworth Cengage Learning.

Kappelman J. 1996. The evolution of body mass and relative brain size in fossil hominids. J Hum Evol 30:243–276.

Keates SG. 2003. Biostratigraphy, taphonomy, palaeoenvironment and hominid diet in the Middle and Late Pleistocene of China. In: Chen S, Keates SG, editors. Current research in Chinese Pleistocene archaeology. Oxford: Archaeopress. p 37– 56.

Kennedy GE. 1990. On the autapomorphic traits of *Homo erectus*. J Hum Evol 20:375–412.

Kennedy KAR, Sonakia A, Chiment J, Verma KK. 1991. Is the Narmada hominid an Indian *Homo erectus*? Am J Phys Anthropol 8 6:475–496.

Key CA, Aiello LC, Molleson T. 1994. Cranial suture closure and its implications for age estimation. Int J Osteoarchaeol 4:193–207.

Kimbel WH, White TD, Johanson DC. 1984. Cranial morphology of *Australopithecus afarensis*: a comparative study based on a composite reconstruction of the adult skull. Am J Phys Anthropol 64:337–388.

Kukla G. 1987. Loess stratigraphy in central China. Quat Sci Rev 6:191–219.

Lahr MM. 1996. The evolution of modern human diversity: a study of cranial variation. Cambridge: Cambridge University Press.

Liu W, Wu X. 2011. The hominid fossils from China contemporaneous with the Neanderthals and some related studies. In: Condemi S, Weniger G-C, editors. Continuity and discontinuity in the peopling of Europe. Dordrecht: Springer Netherlands: . p 77–87.

Maddux SD. 2011. A quantitative assessment of infraorbital morphology in *Homo*: testing for character independence and evolutionary significance in the human midface [Ph.D.]. Iowa City: University of Iowa.

Maddux SD. 2012. A quantitative assessment of zygomaticoalveolar crest curvature in recent and fossil *Homo*. Am J Phys Anthropol 54S:199.

Maddux SD, Franciscus RG. 2009. Allometric scaling of infraorbital surface topography in *Homo*. J Hum Evol 56:161–174.

Manzi G. 2004. Human evolution at the Matuyama-Brunhes boundary. Evol Anthropol 13:11–24.

Manzi G. 2011. Before the emergence of *Homo sapiens*: overview on the Early-to-Middle Pleistocene fossil record (with a proposal about *Homo heidelbergensis* at the subspecific level). Int J Evol Biol 2011:11.

Manzi G, Gracia A, Arsuaga J-L. 2000. Cranial discrete traits in the Middle Pleistocene humans from Sima de los Huesos (Sierra de Atapuerca, spain). Does hypostosis represent any increase in "ontogenetic stress" along the Neanderthal lineage? J Hum Evol 38:425–446.

Manzi G, Mallegni F, Ascenzi A. 2001. A cranium for the earliest Europeans: phylogenetic position of the hominid from Ceprano, Italy. Proc Natl Acad Sci USA 98:10011–10016.

Martin R, Saller K. 1957. Lehrbuch der anthropologie. Stuttgart: G. Fischer.

Martínez I, Arsuaga J-L. 1997. The temporal bones from Sima de los Huesos Middle Pleistocene site (Sierra de Atapuerca, Spain). A phylogenetic approach. J Hum Evol 33:283–318.

Maureille B. 1994. La face chez *Homo erectus* et *Homo sapiens*: recherche sur la variabilité morphologique et métrique [Dissertation]. Talence, France: University of Bordeaux 1.

McKern TW, Stewart TD. 1957. Skeletal changes in young American males. Analyzed from the standpoint of age identification. Environmental Protection Research Division (U.S. Army Quartermaster Research and Development Command), Technical Report EP-45, Natick, US Army.

Meindl RS, Lovejoy CO. 1985. Ectocranial suture closure: a revised method for the determination of skeletal age at death based on the lateral-anterior sutures. Am J Phys Anthropol 68:57–66.

Mounier A, Marchal F, Condemi S. 2009. Is *Homo heidelbergensis* a distinct species? New insight on the Mauer mandible. J Hum Evol 56:219–246.

Norton CJ, Braun DR, Jin C, Wang Y, Zhang Y. 2010. Rethinking the Palearctic-Oriental biogeographic boundary in Quaternary China. In: Norton CJ, Braun DR, editors. Asian paleoanthropology: from Africa to China and beyond. Dordrecht: Springer. p 81–100.

Pearson OM. 2008. Statistical and biological definitions of "anatomically modern" humans: suggestions for a unified approach to modern morphology. Evol Anthropol 17:38–48.

Pérez P-J, Gracia A, Martinez I, Arsuaga JL, 1997 Paleopathological evidence of the cranial remains from the Sima de los Huesos Middle Pleistocene site (Sierra de Atapuerca, Spain). Description and preliminary inferences. J Hum Evol 33:409–421.

Pope GG. 1991. Evolution of the zygomaticomaxillary region in the genus *Homo* and its relevance to the origin of modern humans. J Hum Evol 21:189–213.

Pope GG. 1992. Craniofacial evidence for the origin of modern humans in China. Yearb Phys Anthropol 35:243–298.

Qi G. 1989. Quaternary mammalian faunas and environment of fossil humans in north China. In: Wu R, Wu X, Zhang S, editors. Early humankind in China. Beijing: Science Press. p 237–337. (In Chinese with English abstract).

Qiu Z, Gu Y, Zhang Y, Zhang S. 1973. New discovery of the fossils and cultural remains of *Sinanthropus pekinensis* from Zhoukoudian. Vertebr Palasiat 11:109–131 (in Chinese).

Rightmire GP. 1985. The tempo and change in the evolution of Mid-Pleistocene *Homo*. Ancestors: the hard evidence. New York: Alan R. Liss, Inc. p 255–264.

Rightmire GP. 1990. The evolution of *Homo erectus:* comparative anatomical studies of an extinct human species. Cambridge: Cambridge University Press.

Rightmire GP. 1996. The human cranium from Bodo, Ethiopia: evidence for speciation in the Middle Pleistocene? J Hum Evol 31:21–39.

Rightmire GP. 1998a. Evidence from facial morphology for similarity of Asian and African representatives of *Homo erectus*. Am J Phys Anthropol 106:61–85.

Rightmire GP. 19981998b. Human evolution in the Middle Pleistocene: the role of *Homo heidelbergensis*. Evol Anthropol 6:218–227.

Rightmire GP. 2004. Brain size and encephalization in early to Mid-Pleistocene *Homo*. Am J Phys Anthropol 124:109–123.

Rightmire GP. 2007. Later Middle Pleistocene *Homo*. In: Henke W, Tattersall I, editors. Handbook of paleoanthropology. Berlin; Heidelberg: Springer. p 1695–1715.

Rightmire GP. 2008. *Homo* in the Middle Pleistocene: hypodigms, variation, and species recognition. Evol Anthropol 17:8–21.

Rightmire GP. 2009. Middle and later Pleistocene hominins in Africa and southwest Asia. Proc Natl Acad Sci USA 106:16046–16050.

Rightmire GP, Lordkipanidze D, Vekua A. 2006. Anatomical descriptions, comparative studies and evolutionary significance of the hominin skulls from Dmanisi, Republic of Georgia. J Hum Evol 50:115–141.

Rosenberg KR, Zune L, Ruff CB. 2006. Body size, body proportions, and encephalization in a Middle Pleistocene archaic human from northern China. Proc Natl Acad Sci USA 103:3552–3556.

Rouvière H. 1954. Anatomie humaine, Vol. 1: Tête et cou. Paris: Masson.

Santa Luca AP. 1980. The Ngandong fossil humans: a comparative study of a Far Eastern *Homo erectus* group. New Haven: Yale University Press.

Schick KD, Zhuan D. 1993. Early Paleolithic of China and eastern Asia. Evol Anthropol 2:22–35.

Schwartz JH, Tattersall I. 2003. The human fossil record: craniodental morphology of genus *Homo* (Africa and Asia) New York: Wiley-Liss.

Spitery J. 1982. La face de l'homme de tautavel. Nice: 1<sup>er</sup> Congrès International de Paléontologie Humaine.

Steele DG, Bramblett CA. 1988. The anatomy and biology of the human skeleton. College Station: Texas A&M University Press.

Stringer CB. 1981. The dating of European Middle Pleistocene hominids and the existence of *Homo erectus* in Europe. L'Anthropologie (Paris) 19:3–14.

Stringer CB. 1983. Some further notes on the morphology and dating of the Petralona hominid. J Hum Evol 12:731–742.

Stringer CB. 1984. The definition of *Homo erectus* and the existence of the species in Africa and Europe. Cour Forschungs Senck 69:131–143.

Stringer CB. 1990. The Asian connection. New Scientist 178:33–37.

Stringer C. 2012. The status of *Homo heidelbergensis* (Schoetensack 1908). Evol Anthropol 21:101–107.

Stringer CB, Howell FC, Melentis JK. 1979. The significance of the fossil hominid skull from Petralona, Greece. J Archaeol Sci 6:235–253.

Tattersall I, Schwartz J. 2006. The distinctiveness and systematic context of *Homo neanderthalensis*. In: Harvati K, Harrison T, editors. Neanderthals revisited: new approaches and perspectives. Dordrecht: Springer. p 9–22.

Terhune CE, Deane AS. 2008. Temporal squama shape in fossil hominins: relationships to cranial shape and a determination of character polarity. Am J Phys Anthropol 137:397–411.

Terhune CE, Kimbel WH, Lockwood CA. 2007. Variation and diversity in *Homo erectus*: a 3D geometric morphometric analysis of the temporal bone. J Hum Evol 53:41–60.

Trinkaus E. 1983. The Shanidar Neandertals. New York: Academic Press.

Trinkaus E. 1987. The Neandertal face: evolutionary and functional perspectives on a recent hominid face. J Hum Evol 16:429–443.

Vallois HV. 1969. Le temporal Néanderthalien h 27 de La Quina. Étude anthropologique. L'Anthropologie (Paris) 735–6:365–400.

Wang Y, Xue X, Jue L, Zhao J, Liu S. 1979. Discovery of the Dali fossil man and its preliminary study. Kexue Tongbao 24:303–306 (in Chinese).

Weidenreich F. 1937. The relation of *Sinanthropus pekinensis* to *Pithecanthropus*, *Javanthropus* and Rhodesian man. J R Anthropol Inst Great Britain Ireland 67:51–65.

Weidenreich F. 1943. The skull of *Sinanthropus pekinensis*: a comparative study on a primitive hominind skull. Pehpei, Chungking: Geological Survey of China.

Weidenreich F. 1951. Morphology of Solo man. New York: American Museum of Natural History.

White TD, Folkens PA. 2000. Human osteology. San Diego: Academic Press.

Wolpoff M. 1980. Cranial remains of Middle Pleistocene European hominids. J Hum Evol:339–358.

Wolpoff MH. 1971. Vertesszöllös and the Presapiens theory. Am J Phys Anthropol 35:209–215.

Wu R, Dong X. 1982. Preliminary study of *Homo erectus* remains from Hexian, Anhui. Acta Anthropol Sinica 1:2–13 (in Chinese with English abstract).

Wu X. 1981. A well-preserved cranium of an archaic type of early *Homo sapiens* from Dali, China. Sci Sin 24:530–542.

Wu X. 1988. The place of Maba man in human evolution. Treatises in commemoration of the 30th anniversary of the discovery of the Maba human cranium. Guangdong Provincial Museum and the Museum of Qujiang County, Beijing: Cultural Relics Publishing House. p 3–7 (in Chinese).

Wu X. 1990. The evolution of humankind in China. Acta Anthropol Sinica 9:312–321 (in Chinese with English abstract).

Wu X. 2004. On the origin of modern humans in China. Quat Intl 117:131–140.

Wu X. 2009. A metrical study of the Dali cranium. Acta Anthropol Sinica 28:217–236 (in Chinese with English abstract)

Wu X, Poirier FE. 1995. Human evolution in China: a metric description of the fossils and a review of the sites. New York: Oxford University Press.

Wu X, You Y. 1979. A preliminary observation of the Dali man site. Vertebr Palasiat 17:294–303 (in Chinese with English abstract).

Wu XJ, Schepartz LA, Liu W, Trinkaus E. 2011. Antemortem trauma and survival in the Late Middle Pleistocene human cranium from Maba, south China. Proc Natl Acad Sci USA 108: 19558–19562.

Wu XJ, Trinkaus E. In press. Neurocranial trauma on the late archaic human remains from Xujiayao, northern China Int J Osteoarchaeol.

Xiao J, Jin C, Zhu Y. 2002. Age of the fossil Dali man in north-central China deduced from chronostratigraphy of the loess-paleosol sequence. Quat Sci Rev 21:2191–2198.

Yin G, Zhao H, Yin J, Lu Y. 2002. Chronology of the stratum containing the skull of the Dali man. Chinese Sci Bull 47:1302–1307.

Zhang SS, Zhou CM. 1984. A preliminary study of the second excavation of Dali man locality. Acta Anthropol Sinica 3:19–31 (in Chinese).